Evaluation of non-Rutherford proton elastic scattering cross section for magnesium

A.F. Gurbich [a,*], C. Jeynes [b]

[a] *Institute of Physics and Power Engineering, Obninsk, 249020, Russia*

[b] *University of Surrey Ion Beam Centre, Guildford, GU2 7XH, England*

[*]Corresponding author: A.F.Gurbich
Address: Bondarenko sq., 1,
Institute of Physics and Power Engineering,
249020, Obninsk,
Russian Federation
Fax: +7 08439 58477
Tel: +7 08439 94169
E-mail: gurbich@ippe.ru

Abstract

The experimental data available for magnesium (p,p) elastic scattering cross section at angles and energies suitable for Ion Beam Analysis have been evaluated using the theoretical model approach together with additional measurements and benchmark experiments. The results obtained provide the evaluated differential cross sections for magnesium (p,p) elastic scattering in the energy region up to 2.7 MeV.

Key words: proton elastic scattering, magnesium, cross section, evaluation

PACS: 25.40.Cm

1. Introduction

This article continues a series of papers devoted to the evaluation of non-Rutherford cross sections for Ion Beam Analysis (IBA). The results achieved so far are summarized in [1]. It was demonstrated that the evaluation of the cross sections by combining different sets of experimental data in the framework of a theoretical model makes it possible to calculate the smooth curves of $d\Omega/d\theta(E,\theta)$ needed for simulation of IBA spectra with a reliability exceeding that of any individual measurement.

The evaluation procedure consists of the following: Firstly, a search of the literature and of nuclear data bases is made to compile and compare relevant experimental data. The apparently reliable experimental points are critically selected. Free parameters of the theoretical model, which involve appropriate physics for the given scattering process, are then fitted within the limits of reasonable physical constraints. Details of the physics are described elsewhere [2]. Additional experimental data can be incorporated *a posteriori*. If necessary, benchmark experiments are performed to arbitrate discrepancies.

Magnesium is an important element. It is the crucial component of, for example, light strong metal alloys important for aerospace structural materials and certain automotive components. In any application where thin film coatings or tribological layers are investigated we may expect the ability to use IBA to be useful.

Magnesium diboride is also an interesting new superconductor with a critical temperature of 39K. Rutherford backscattering (RBS) has been used to determine the elemental depth profile in ion beam synthesised MgB_2 [3], but the sensitivity to B is poor in RBS. An alternative approach is to use elastic (non-Rutherford) backscattering (EBS) where the sensitivity to B is enhanced by an order of magnitude for a 2.6MeV beam. However, at this proton energy the elastic scattering cross-section for Mg is also strongly non-Rutherford, and must be determined for EBS depth profiling to be used.

In this work, we have identified a discrepancy between the *a priori* most likely theoretical excitation function (elastic scattering cross-section) for Mg, and existing data in the region 850-1250 keV, just above the first resonance at 823keV. Additional benchmarking measurements on both thin and thick films have supported the theoretical function.

2. Evaluation

The differential proton elastic scattering cross sections for magnesium in the energy range from Coulomb scattering to 2.5 MeV were found in four papers: Mooring *et al* (1951) [4], Rauhala *et al* (1988) [5], Zhang *et al* (2003) [6], and Wang *et al* (1972) [7]. The reported data were measured at laboratory angles of 164.5° (Mooring), 170° (Rauhala), 140°, 150°, 160°, 170° (Zhang), and 130°,150° (Wang) in the energy range of 0.40-3.95, 0.8-2.7, 0.8-2.5, and 1.5-3.0 MeV respectively. Natural magnesium (78.99% of ^{24}Mg, 10.00% of ^{25}Mg, and 11.01% of ^{26}Mg) was used for manufacturing targets in Rauhala and Zhang, the target material in Mooring was $^{24}MgF_2$ enriched by the ^{24}Mg isotope up to 99.50%, and the target in Wang was also of high enrichment (~99%). The measurements reported in Mooring, Zhang and Wang were made with thin targets prepared by evaporation of magnesium onto graphite backing and with a thick sample in Rauhala. A computer fit using the simulation program GISA [8] and TRIM77 [9] stopping powers for Mg provided the cross sections in the last case. The spectra of elastically scattered protons were measured by means of a magnetic analyzer (Mooring) and with silicon surface barrier detectors for all the others. A large background scattering from the impurities contained in the graphite backing was found in Mooring and the corresponding correction was made for the cross-section determination.

For Zhang, the absolute values of differential cross sections were determined assuming that the scattering was Rutherford below 0.8 MeV. The absolute normalization was made against the yield of protons elastically scattered from the Au layer evaporated on the Mg one. The experimental standard error assigned to the data in was 5%. The target thickness in Wang was determined by assuming that the scattering was Rutherford near 1 MeV and the total experimental uncertainty was estimated to be about 10%.

The absolute normalization in Rauhala was made in a similar way as in Zhang and the error assigned to the data was estimated to be less than 5% including inaccuracies due to possible errors in the stopping powers which were used in order to determine the cross section from the relative backscattering yields of Au and Mg. The estimate of 5% in Rauhala depends on the reliability of the shape of the stopping power curve since the absolute yields are all interpreted relative to the Rutherford regime below 800keV. However Ziegler's more recent SRIM2003 estimates of stopping power (www.srim.org)

have a *ratio* between the values at 778keV and 1216keV that are more than 3% different from those Ziegler *et al* published in 1985 [10] (the stopping power for H in Mg is (8.93 & 6.74) eV/(10^{15} atoms/cm^2) for TRIM90 and (8.30 & 6.47) eV/(10^{15} atoms/cm^2) for SRIM03 with proton energies of (776 & 1216) keV respectively).

For the sake of completeness Valter *et al* (1963) [11] should also be mentioned. The differential cross sections for ^{24}Mg(p,p$_0$)^{24}Mg were measured at 90°, 125° and 141° (c.m.) from 1.45 to 4.20 MeV. Unfortunately the data were only presented for energies above 2.7 MeV.

As a whole, the data obtained are in a reasonable mutual agreement and some differences caused by the different isotopic content of the targets employed are observed between the data of Rauhala and Zhang, and the earlier work of Mooring and Wang on isotopically enriched targets.

The differential scattering cross section function is Rutherford below ~800 keV and shows several scattering anomalies at higher energies (Fig. 1). A remarkable feature of the curve discovered in Mooring was that on the low energy side of the narrow 0.823 MeV resonance the observed cross section values followed closely the expected Coulomb scattering, whereas on the high energy side it was found to be about 10% higher. Since the data below and above 0.85 MeV were taken in Mooring with different targets, the authors made additional efforts to confirm the result and they claimed that the reported deviation from Rutherford scattering above the 0.823 MeV resonance was real. A similar ~10% excess of the cross section over the Rutherford value above the 0.823 MeV resonance was obtained also by both Rauhala and Zhang for the differential cross sections measured at different scattering angles with exception of the results for 150° reported by Zhang (Fig. 2).

It is known that broad shape resonances may significantly influence the cross section [12]. The fact that the l=4 Legendre polynomial is zero at the scattering angle of 149.27° c.m. could in principle account for the dip in the angular distribution at the 150° scattering angle measured in Zhang. However, this can be ruled out since the contribution of this partial wave to the cross section is negligible because of its extremely small transmission coefficient at low energy.

Theoretical calculations in the present work were made in the framework of the R-matrix theory of Lane & Thomas (1958) [13]. The formulae (2.6)-(2.7) of sect. VIII of this reference were programmed for the one channel multilevel case. The cross section for natural magnesium was calculated as a sum of the cross sections for its three stable isotopes weighted by the relative abundance. The resonance parameters were taken from the compilation of Endt & van der Leun (1973) [14]. The general trend of the observed cross sections, including resonances, was well reproduced theoretically (see Fig.1). The theoretical analysis was facilitated by the previous investigation of Koester (1952) [15] where the energy dependence of the cross section for ^{24}Mg(p,p$_0$)^{24}Mg measured by Mooring was interpreted in terms of the combination of Coulomb and nuclear potential scattering with resonant scattering. This resonant scattering arises from the excitation of energy levels of the compound nucleus ^{25}Al. In the case of proton scattering from natural magnesium the excitation of the ^{26}Al and ^{27}Al energy levels should also be taken into account. For the p+^{25}Mg scattering a lot of resonances are observed in the excitation function [16], however they are relatively narrow and rather weak. Being weighted accordingly to the isotope abundance the p+^{25}Mg contribution to the natural magnesium cross section is practically indistinguishable and so the corresponding curve is not shown in Fig. 1. The p+^{26}Mg case is another matter [17]. The large anomaly with a peak just above 2 MeV substantially influences the differential cross section for natural magnesium (see Fig. 1) and is responsible for the observed difference in the cross sections for natural magnesium and the ^{24}Mg isotope.

3. Benchmark Measurements

In order to resolve the problem with the cross-section behaviour around the resonance at E_p=823 keV benchmark measurements were made with a thin film target. Proton backscattering spectra above the various resonances were also obtained with a thick uniform natural magnesium target as benchmark measurements to validate the structure of the fine resonances. These measurements were all done using a 2 MV Tandetron capable of generating proton beams up to 4 MeV [18]. This machine has a terminal voltage controlled (with a precision generating voltmeter) with an accuracy better than 0.1%. No slit stabilisation on the analysing magnet is needed (or used).

Surface barrier detectors at scattering angles of 172.8° (Cornell geometry) and 148.2° (IBM geometry) with solid angles of 1.25 and 3.5msr were used simultaneously in the measurements. A Mg foil sample (Goodfellow Metals Ltd.) served as a target. It was 99.9% pure (impurity mostly Fe), 25x25 mm, 0.25 mm thick, as rolled. The surface oxide and

carbon contamination was evaluated (see Fig.3). Beam current was ~10 nA, nominal beam size (normal incidence) was 1 mm. A second test sample was a Au/Mg multilayer on vitreous carbon, sputter deposited by Teer Coatings Ltd, and containing (270, 958, 371).10^{15}/cm^2 of (Au, Mg, O) respectively.

The electronics calibration was made with a Au/Ni/SiO_2/Si sample (see [19]), using Lennard's pulse height defect (PHD) correction for the non-ionising energy loss [20] and an assumed surface electrode thickness of (246, 100).10^{15} Au/cm^2 for the A and B detectors respectively (equivalent to (80, 32.5)μg/cm^2 or (42, 17)nm, including dead layer). The average offset determined for the whole energy range with fixed gain was (-6.5±0.8, -3.5±0.7)keV for the two detectors, where the uncertainty given is the standard error. This offset is equivalent to (1.4, 0.8) channels in the MCAs (multichannel analysers). The gain had an apparent uncertainty (standard error over the whole dataset) of less than 0.1%. Without the PHD correction the apparent gain changes by 5% across the energy range. This would be enough to destroy the relative energy correlations of the spectra. With the PHD correction we can compare the energies of the various resonances since the gain is constant across the whole dataset. Determination of electronic gain at comparable precision is reported by Bianconi *et al* (2000 [21], see Barradas *et al* 2007, [22]) and Munnik *et al* (1995 [23]).

The DataFurnace code (NDFv8.1h) [24, 25] was used to calculate the spectra from the excitation function. Unless both the straggling and the convolution of the straggling and the cross-section function are calculated correctly, the spectral shape for buried resonances will not be properly reproduced. DataFurnace has new algorithms to handle non-Rutherford cross-sections correctly. The number of internal calculation layers is determined by the cross-section data file [26]. This is essential for correct interpolation since the system resolution (~14keV) is often much larger than the the width of resonances (for example, the 1483keV resonance has a FWHM of only 400eV). Also, the effect of the energy spread before interaction is large for sharp resonances, and is now correctly taken into account by the DataFurnace code [27]. The "DEPTH" code of Szilágyi [28] was used to correctly determine the effect of straggling on the effective energy resolution as a function of depth.

The accurate pulse pileup correction algorithm of Wielopolski & Gardner [29] was used to maintain the accuracy of the cross-section measurements on the thin film sample [30]. The pileup correction can exceed 3% for the larger detector, and we emphasise that this is a non-linear correction (the pileup-corrected Au signal is *larger* than the measured signal since counts are lost from the peak) and is calculated without free parameters using the amplifier shaping time (500ns), and the time resolutions of the pileup rejection circuit, which were (520, 550)ns for the two detection channels. In fact the PUR time resolutions were adjusted slightly from the expected 500ns to match the observed pileup probability. The W&G algorithm is exact for 2-pulse pileups, but was extended in the DataFurnace code to give an approximate estimate of 3-pulse pileups. These were negligible in this work.

The pileup calculation is an interative convolution of the observed spectrum with itself. This has the disadvantage that the part of the spectrum below the LLD (lower level discriminator) of the MCA is unobserved. This means that the pileup cannot be calculated correctly near leading edges in the spectrum since the low energy pulses are missing from the spectrum. In the case that there is significant electronic noise in a detection channel this may be a significant effect. For the present data for the Au/Mg ML sample, there is a noticeable high energy tail on the Au signal which is attributable to pileup from the low energy part of the spectrum (below the LLD). We have simulated low energy "noise" to roughly account for this since it is important to have an accurate estimate of the real (pileup corrected) number of Au counts. In these data the calculated pileup correction is large: it *increased* the apparent Au signal by up to 3.3% and *decreased* the apparent Mg signal by up to 4.5%

Fig. 3 directly compares the scattering cross-sections proposed here with the experimental data for the bulk Mg sample, near the 823, 1483 and 1630 keV resonances. It is clear that the data are well reproduced by the SigmaCalc cross-sections, even at the sharp resonance at 1483keV which is not well determined by Moore's cross-section measurement because the Mg thin films used are too thick. The bulk data determines the height of the resonance, given the resonance width. The real cross-sections derived from the fitted resonance parameters can be folded with the target thickness and the beam width given by Moore to recover the measured cross-sections (see Fig.4)

Table 1 shows the analysis of the Au/Mg sample, where results are given relative both to the Rutherford Au signal, and to the C substrate, using evaluated (SigmaCalc) C cross-sections [31]. , Evaluated (SigmaCalc) cross-sections are also used for the O contaminant [32]. The sample structure was first determined in the Rutherford region, and then the spectra at different energies were simulated, and the apparent Au and Mg thicknesses determined by comparison of the data with the simulations. If the SigmaCalc cross-sections are correct the Au and Mg thicknesses should be constant. The Table shows the quality of the data, with the counting statistics uncertainty and the standard error of the estimated Au and Mg thicknesses calculated separately. The Mg thickness relative to both the carbon substrate and the Rutherford Au signal is

also shown, and the two detectors are compared. The latter clearly shows that the detectors are strongly correlated. These data are summarised in Fig.5.

5. Conclusion

The proton elastic scattering from natural magnesium has been evaluated, and can now be reliably calculated for any scattering angle in the energy range from Coulomb scattering up to 2.7 MeV. The uncertainty of SigmaCalc cross-sections proved to be not worse than 2%.

It is shown that sharp strong resonances observed in the cross-section are also prominent in thick targets. For example, the full structure of the strong resonance at 1483keV was not reproduced in any reported thin target measurement, but a correct simulation using the theoretical cross-sections reproduced the data well.

The evaluated elastic scattering cross-sections are available from http://www-nds.iaea.org/sigmacalc mirrored at http://www.surreyibc.ac.uk/sigmacalc.

Acknowledgments

One of the authors (A.G.) is grateful to colleagues from the University of Surrey Ion Beam Centre for warm hospitality, and to the Royal Society for support under the Incoming Short Visit programme for 2005. We are grateful to Kevin Cooke of Teer Coatings Ltd. for depositing the Au/Mg multilayer sample. The work was supported by EPSRC under contract GR/R50097/01.

Figure captions

Fig. 1. The evaluated differential cross sections and the available experimental data for proton elastic scattering from magnesium (the experimental points from Ref. [2] were thinned out in order not to obscure the figure).

Fig. 2. The angular distribution of protons elastically scattered from magnesium at energy above the 0.823 MeV resonance, SigmaCalc compared with the literature.

Fig. 3. Data and simulations for a bulk Mg sample near the a) 823, b) 1483 and c) 1630keV resonances. Scattering angle 172.8°.

Fig.4 1483keV resonance in absolute (SigmaCalc) and experimental (Moore and folded) representation

Fig.5: Apparent Mg content of multilayer sample, normalised to Rutherford Au signal, extracted from Table 1 for the $^{Nat}Mg(p,p)^{Nat}Mg$ reaction. The ordinate is in units of 10^{15}atoms/cm^2 (TFU). ±2% uncertainty bars are shown. NDFv8.1h [16] is used with SRIM2003 electronic stopping powers [www.srim.org]

Table Captions

Table 1: Pileup corrected data quantified by comparison with simulation

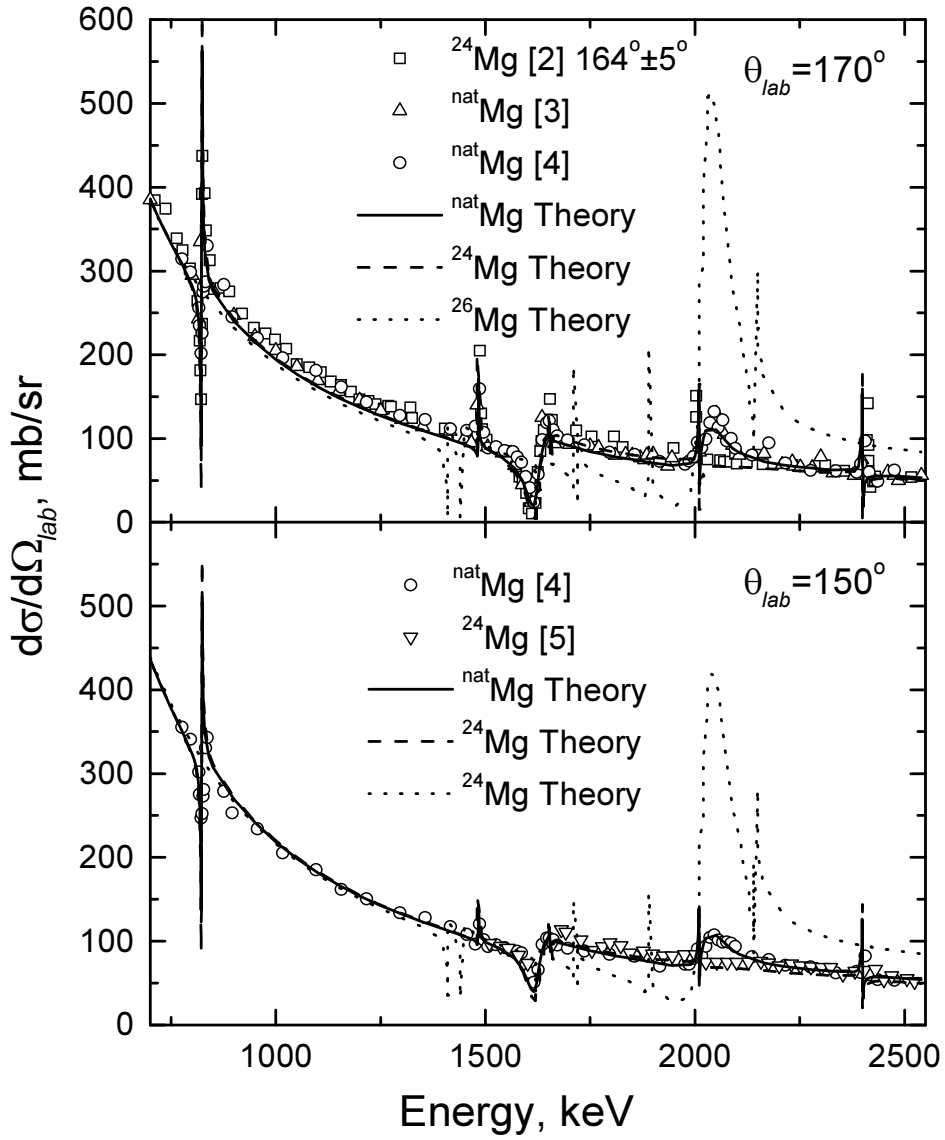
600
500
400
300
200
100
0
^{24}Mg [2] 164°±5°
^{nat}Mg [3]
^{nat}Mg [4]
^{nat}Mg Theory
^{24}Mg Theory
^{26}Mg Theory
θ_{lab}=170°
^{nat}Mg [4]
^{24}Mg [5]
^{nat}Mg Theory
^{24}Mg Theory
^{24}Mg Theory
θ_{lab}=150°
1000
1500
2000
2500
Energy, keV
dσ/dΩ$_{lab}$, mb/sr

Fig. 1

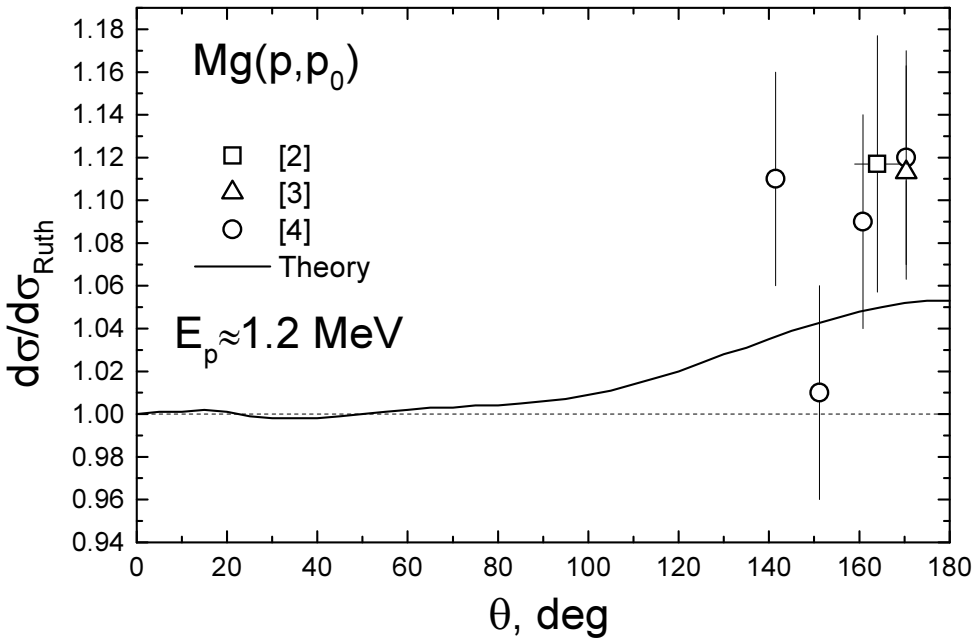
Mg(p,p0)
[2]
[3]
[4]
Theory
Ep≈1.2 MeV
dσ/dσRuth
θ, deg
1.18
1.16
1.14
1.12
1.10
1.08
1.06
1.04
1.02
1.00
0.98
0.96
0.94
0
20
40
60
80
100
120
140
160
180

Fig. 2

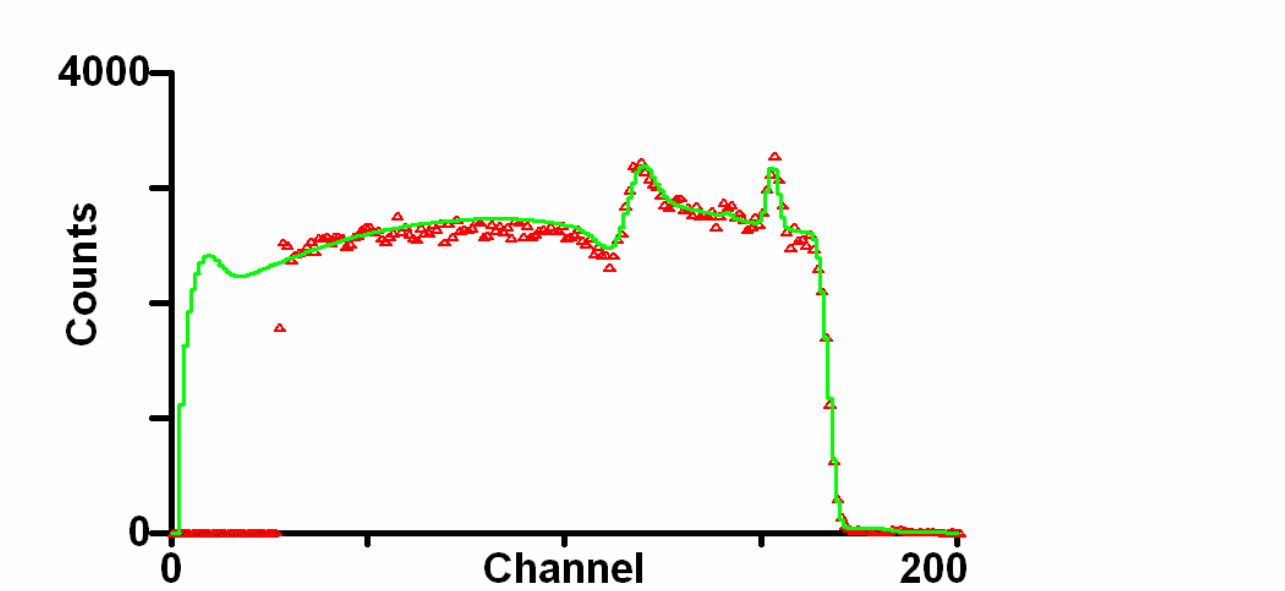

Fig.3a) 942.5keV. Around ch.90 the simulation is 3% higher than the data

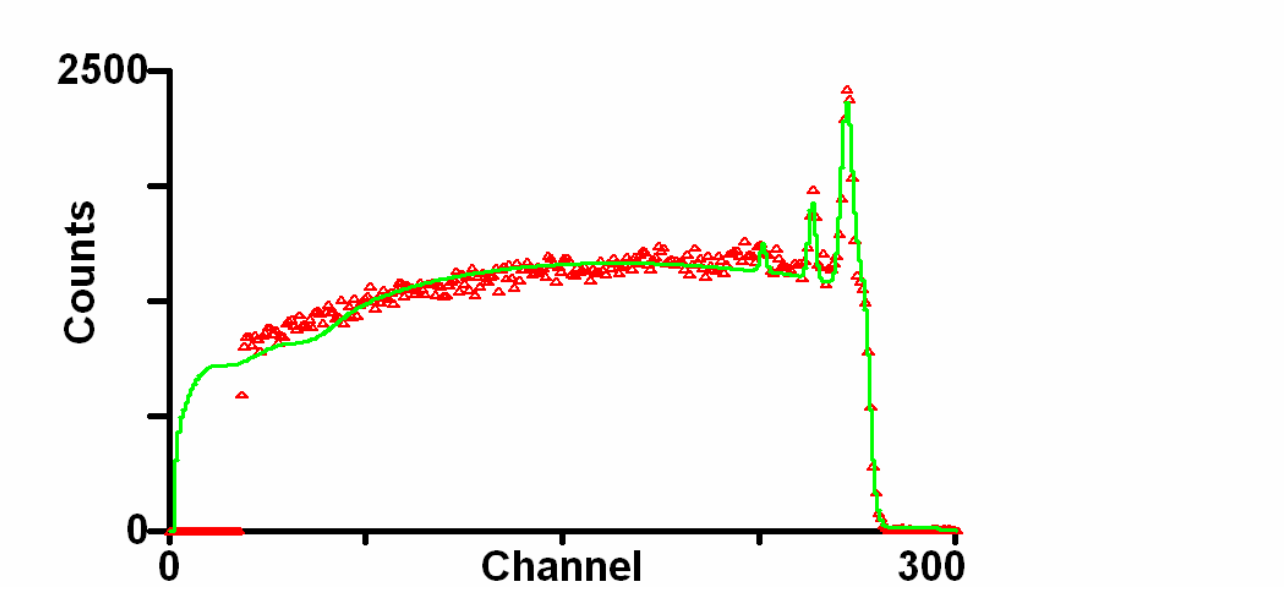

Fig.3b) 1506keV

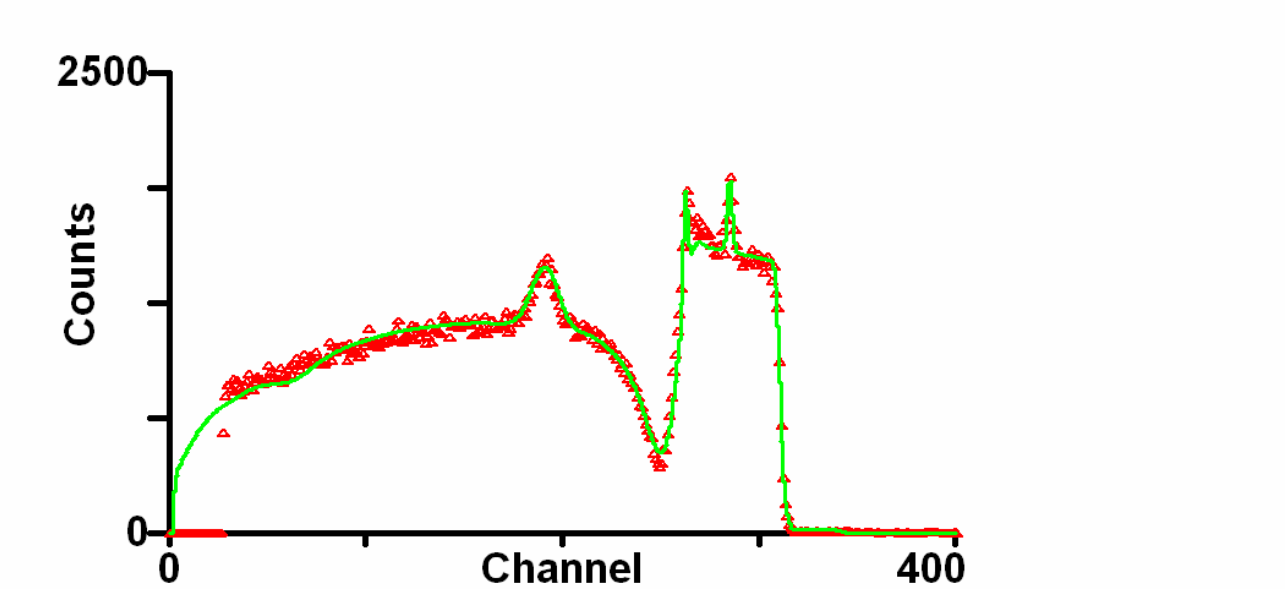

Fig.3c) 1752keV

Fig 3: Spectra from Mg bulk sample with proton beam energies 942.5, 1506, 1752 keV and 172° scattering angle. There is 68.10^{15} C/cm^2 and 800.10^{15} MgO/cm^2 on the surface

Table 1: Pileup corrected data quantified by comparison with simulation

Thickness given in thin film units (TFU: 10^{15}atoms/cm^2). Detectors A and B have scattering angles 172.8^0 and 148.2^0

	Energy	Au		Mg		O		Average Mg		Au	Mg	O
		A det	Bdet	A det	Bdet	A det	Bdet	norm: C	norm: Au	A/B	A/B	A/B
	keV	TFU	TFU	TFU	TFU	TFU	TFU	TFU	TFU			
1	**706.75**	278	271	976	959	377	386	**968**	968	1.026	1.018	0.976
2	**706.75**	281	274	967	994	399	398	**981**	969	1.025	0.973	1.004
3	**840**	279	269	976	951	354	369	**964**	964	1.037	1.026	0.960
4	**942.5**	281	268	969	929	318	355	**949**	947	1.047	1.043	0.896
5	**1147.5**	283	272	998	933	303	307	**965**	955	1.041	1.069	0.986
6	**1352.5**	285	273	958	930	321	315	**944**	928	1.043	1.030	1.021
7	**1506**	285	275	959	914	322	293	**937**	917	1.035	1.050	1.099
8	**1506**	288	275	942	927	313	295	**935**	911	1.050	1.016	1.062
9	**1752**	280	273	1010	989	308	306	**1000**	991	1.025	1.021	1.008
10	**840**	280	271	964	940	361	369	**952**	947	1.035	1.025	0.978
Uncertainty		0.3%	0.2%	1.2%	0.7%	2.3%	1.3%	1.3%	1.4%	0.4%	1.3%	2.7%
Average		282	272	972	947	338	339	959	950	1.037	1.027	0.999
Standard deviation		**1.1%**	**0.8%**	**2.0%**	**2.8%**	**9.7%**	**11.8%**	**2.3%**	**2.6%**	**0.9%**	**2.5%**	**5.6%**

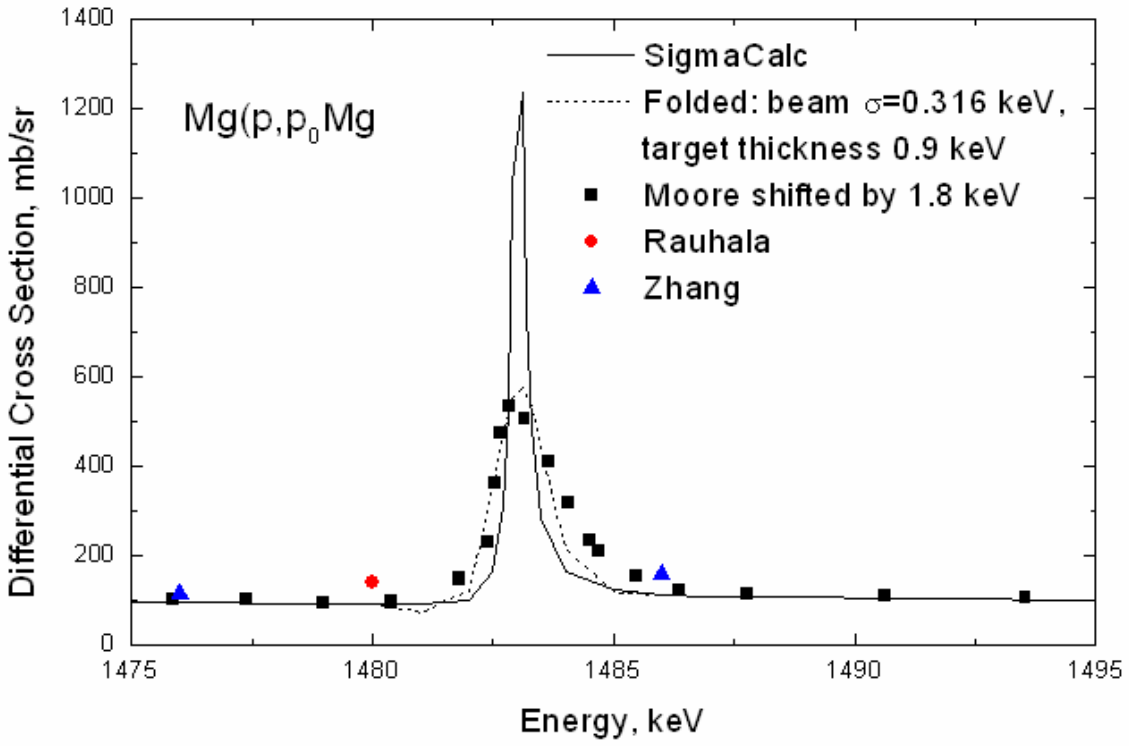

Fig.4: 1483keV resonance in absolute (SigmaCalc) and experimental (Moore and folded) representation

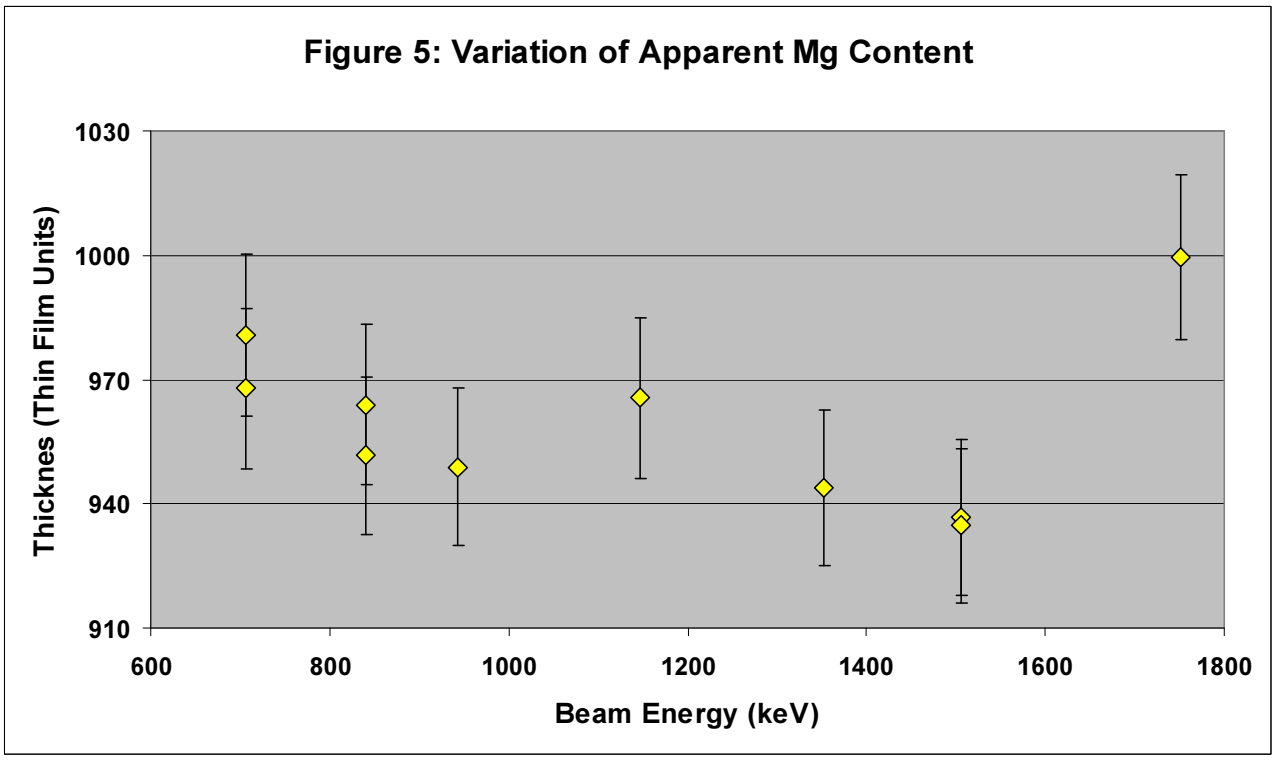

Fig.5: Apparent Mg content of multilayer sample, normalised to the substrate signal, extracted from Table 1 for the $^{Nat}Mg(p,p)^{Nat}Mg$ reaction. The ordinate (TFU) is in units of 10^{15}atoms/cm^2. ±2% uncertainty bars are shown.

References

1 A.F. Gurbich, in: R.C. Haight, M.B. Chadwick, T. Kawano, P. Talou (Eds.) Nuclear Data for Science and Technology, AIP Conf. Proc. vol. 769, Melville, New York, 2005, p. 1670.

2 Gurbich 2006 (CAARI 2006 conf.)

3 N.P.Peng, G.Shao, C.Jeynes, R.P.Webb, R.M.Gwilliam, G.Boudreault, D.M.Astill, W.Y.Liang, Appl.Phys.Lett. 82 (2): 236-238 JAN 13 2003

4 F.P. Mooring, L.J. Koster, E. Goldberg, D. Saxon, S.G. Kaufmann, Phys. Rev. 84 (1951) 703

5 E. Rauhala, M. Luomajärvi, Nucl. Instr. and. Meth. B 33 (1988) 628

6 X. Zhang, G. Li, B. Ding, Z. Liu, Nucl. Instr. and Meth. B 201 (2003) 551

7 W.N. Wang, E.K. Lin, C.L. Tung, Chinese Journal of Physics, 10 (1972) 1

8 E.Rauhala, J.Appl.Phys. 62 (1987) 2140

9 H.H. Andersen and J.F. Ziegler. Hydrogen - Stopping Powers and Ranges in All Elements, vol. 3 of The Stopping and Ranges of Ions in Matter. Pergamon Press, New York, 1977

10 J.F. Ziegler, J.P. Biersack, and U. Littmark. The Stopping and Range of Ions in Solids, vol. 1 of The Stopping and Ranges of Ions in Matter. Pergamon Press, New York, 1985

11 A.K. Valter, V.E. Storizhko, A.I. Popov, J. Experimental and Theoretical Phys. 44 (1963) 57 (in Russian)

12 A.F.Gurbich, Nucl. Instr. and Meth. B 217 (2004) 183

13 A.M. Lane, R.G. Thomas, Rev. of Mod. Phys. 30 (1958) 257

14 P.M. Endt, C. Van der Leun, Nucl. Phys. A 214 (1973) 130

15 L.J. Koester, Jr., Phys. Rev. 85 (1952) 643

16 A.I. Popov, P.V. Sorokin, V.E. Storizhko, A.Ya. Taranov, Izvestia Akademiy Nauk SSSR Ser. Fiz. 26 (1962) 1074 (in Russian)

17 C.R. Westerfeldt, G.E. Mitchel, E.G Bilpuch, D.A Outlaw, Nucl. Phys. A 303 (1978) 111

18 A. Simon, C. Jeynes, R.P. Webb, R. Finnis, Z. Tabatabaian, P.J. Sellin, M.B.H. Breese, D.F. Fellows, R. van den Broek, R.M. Gwilliam, Nucl. Instr. and Meth. B 219-220 (2004) 405

19 C. Jeynes, N. P. Barradas, M. J. Blewett, R. P. Webb, Nucl. Instr. and Meth. B 136-138 (1998) 1229

20 W.N.Lennard, S.Y.Tong, G.R.Massoumi, L.Wong, Nuclear Instr. & Methods **B45** (1990) 281-284

21 M.Bianconi, F.Abel, J.C.Banks, A.Climent Font C.Cohen, B.L.Doyle, R.Lotti, G.Lulli, R.Nipoti, I.Vickridge, D.Walsh, E.Wendler, Nucl. Instr. and Methods **B161-163** (2000) 293-296

22 N.P. Barradas, K. Arstila, G. Battistig, M. Bianconi, N. Dytlewski, C. Jeynes, E. Kótai, G. Lulli, M. Mayer, E. Rauhala, E. Szilágyi, M. Thompson (2007), Nucl. Instrum. Methods B (Accepted Manuscript, Available

online 7 June 2007,) (http://www.sciencedirect.com/science/article/B6TJN-4NX8MKX-3/2/afc249c7592de154235d44b406cb3dfd)

23 F. Munnik, A.J.M. Plompen, J. Räisänen, U. Wätjen, (1996), Nucl. Instr. and Methods B119, 445-151

24 N.P. Barradas, C. Jeynes, R.P. Webb, Appl. Phys. Lett. 71 (1997) 291

25 C Jeynes, N P Barradas, P K Marriott, G Boudreault, M Jenkin, E Wendler, R P Webb, *J. Phys. D: Appl. Phys.* **36** R97-R126

26 A.F.Gurbich, N.P.Barradas, C.Jeynes, NIM B190: 237-240 MAY 2002

27 N.P.Barradas, E.Alves, C.Jeynes, M.Tosaki; NIM B247 (2): 381-389 JUN 2006

28 E. Szilágyi, F. Pászti, and G. Amsel, Nucl. Instrum. and Methods B 100 (1995) 103

29 L. Wielopolski, R.P. Gardner, NIM133 (1976) 303

30 N.P.Barradas, M.A.Reis, X-ray spectrometry 35 (4): 232-237 JUL-AUG 2006

31 A.F.Gurbich, Nucl. Instr. and Methods B136-138 (1998) 60

32 A.F. Gurbich, Nucl. Instr. and Meth. B 129 (1997) 311-316